Effect of capping of contaminated sediment by dredged soil with high organic content on leaching of polycyclic aromatic hydrocarbons

Student Number: 07M16037 Name: Naohiro KANEKO

含有機物浚渫泥を用いた覆砂による多環芳香族炭化水素類の溶出防止効果

金子　尚弘

ダイオキシン類，有機スズ化合物（TBT），多環芳香族炭化水素類（PAHs）などの有害物質は，1970年代以降の規制などにより環境中への排出量は減少しているものが多い．しかし，湖沼や沿岸海域の堆積物には依然として高濃度に残留しており，生態系への影響が懸念されている．本研究では，従来有効利用されていない有機物を多く含む浚渫土砂による覆土を施工することによって有害物質溶出低減効果がどの程度期待できるかを明らかにした。代表的疎水性汚染物質としてPAHsに着目し，名古屋港において採取した港湾堆積物を用いてPAHsの吸着実験を行った．また，数値シミュレーションにより，覆土による溶出防止工の長期にわたる効果を予測した．

Key Words :*Polycyclic Aromatic Hydrocarbons, sediment, Nagoya port, adsorption,diffusion*

１．　Introduction

Polycyclic aromatic hydrocarbons, called PAHs, are widely spread by human activities relating on the use of fossil fuel. For instance, Benzo(a)pyrene, one of the PAHs, has an intensive mutagenic and carcinogenic property, and some of PAHs metabolites are known to be endocrine disrupting chemicals [1][2]. Therefore, many studies on the concentration levels of PAHs and on the fate in environments have been carried out to evaluate the PAHs exposure to wild organisms and human being.

The physical-chemical properties of PAHs are widely varied depending on their ring-number. The more ring-number PAHs have higher hydrophobicity, the lower vapor pressure and higher toxicity. In general, PAHs that have more ring-number, are associated with fine particles in environments [3]. Although the emission of PAHs from human activities such as burning fossil fuel are directed to the atomospheric environments, PAHs fall to land surface as dry deposition and wet deposition with fine particles, and are accumulated on road surface and other places. The particles discharged to rivers by runoff in the rainfall events, are eventually transfered to sediments of lakes, bays, harbors and ports [4]. Consequently, benthic organisms in aqueous environments are exposed to PAHs through the foodchain process intaking of fine particles.

In Japan, PAHs are not listed in the environmental quality standards, while PAHs were detected at high levels in sediments. In ports and harbors, PAHs may be transfered by human activities like dredging and soil capping.

In this study, to reduce the leaching of PAHs by the capping with the use of dredged materials with high contents of organic carbon, field observations in Nagoya port were conducted together with adsorption experiments in an anaerobic condition by using sediments obtain from Nagoya port. A one-dimension diffusion model was applied to the data from the field observation and the laboratory experiments to consider the environmental fate of PAHs after the capping in the port.

２．　Field observation

(1) Outline of the field observation

The field observation in Nagoya port was conducted on July 2008. The port area is 83 km^2. The average difference of the tidal level is 1.3m. **Fig.1** shows the sampling points. **Table.1** shows the coordinates of the sampling points.

(2) Result of physical examination of Ngoya port sediment

Ignition loss, composition ratio of clay and silt, total organic carbon, concentration of zinc, cadmium, and benzo(a)pyrene in the soil samples were measured. **Table.2** shows the result of these examinations. Ignition loss , TOC, composition ratio of clay and silt were high around the estuary of Hori river and ship berth. The concentration of zinc and cadmium was high around the estuary of Hori river. Their concentration decreased with the increase in the distance from the Hori river mouse.

Consequently, one of the most dominant sorces of them was the urban runoff. The concentration of benzo(a)pyrene in soil was high near the specific industrial area. The concentration of benzo(a)pyrene decreased with the distance of the contaminated spot. The spacial distribution of organic content, silt and clay ratio, and heavy metals were quite similar, though they were quite different from that of PAHs, reflecting the difference of the sources of the contaminants.

Table 1 Coordinates of sampling points

	Norht latitude	East langitude		Norht latitude	East langitude
No.1	35°05.557′	136°48.705′	No.19	35°03.433′	136°52.917′
No.2	35°05.582′	136°50.470′	No.20	35°02.567′	136°53.667′
No.3	35°05.848′	136°51.828′	No.21	35°01.683′	136°51.483′
No.4	35°06.082′	136°53.678′	No.22	35°02.000′	136°50.783′
No.5	35°05.595′	136°53.870′	No.23	35°01.750′	136°50.167′
No.6	35°05.075′	136°53.790′	No.24	35°01.483′	136°48.650′
No.7	35°04.093′	136°53.795′	No.25	35°00.650′	136°47.650′
No.8	35°04.100′	136°53.133′	No.26	35°00.450′	136°49.350′
No.9	35°05.100′	136°53.433′	No.27	35°01.028′	136°51.107′
No.10	35°05.467′	136°53.217′	No.28	35°00.700′	136°52.217′
No.11	35°05.317′	136°52.217′	No.29	35°00.533′	136°50.800′
No.12	35°04.633′	136°52.750′	No.30	34°59.617′	136°49.700′
No.13	35°04.133′	136°51.733′	No.31	34°59.183′	136°49.400′
No.14	35°04.517′	136°50.750′	No.32	34°58.250′	136°49.367′
No.15	35°04.433′	136°49.867′	No.33	34°56.650′	136°47.683′
No.16	35°03.317′	136°51.050′	No.34	34°59.312′	136°48.006′
No.17	35°03.317′	136°51.933′	No.35	34°58.300′	136°45.800′
No.18	35°02.595′	136°52.123′			

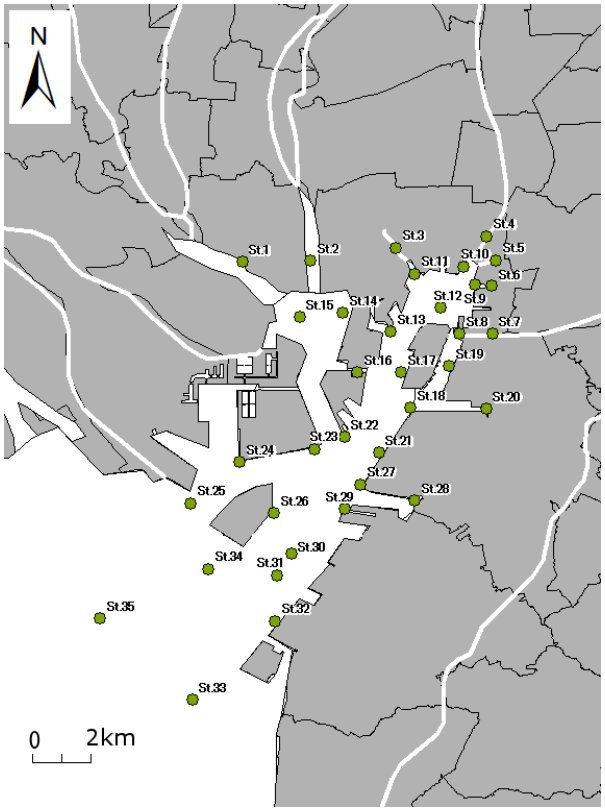

Fig.1 Sampling points in Nagoya port

Table 2 Result of physical examination of Ngoya port sediment

Site	Ignition Loss	Silt+Clay	TOC	Zink	Cadmium	Benzo(a)pyrene
	%	%	mg/g	mg/kg	mg/kg	concentration (ng/g-d
St.1	3.0	63.4	4.78	160	0.30	31.2
St.2	0.9	2.2	0.28	81	0.27	7.2
St.3	15.8	94.2	33.6	2100	2.5	739.6
St.4	14.5	86.8	32.1	2200	6.4	1678.5
St.5	12.7	93.9	21.8	1100	3.8	872.7
St.6	18.3	29.6	32.6	790	12	507.9
St.7	6.1	49.7	12.8	180	0.47	86.8
St.8	1.2	5.4	0.64	64	0.18	27.5
St.9	14.4	90.3	25.1	880	5.7	871.9
St.10	14.2	96.5	34.2	1100	4.1	957.2
St.11	5.7	64.1	9.92	350	1.5	186.2
St.12	10.5	93.5	20.4	820	3.2	686.9
St.13	15.1	93.9	28.9	380	1.1	689.5
St.14	1.0	6.8	0.14	64	0.22	28.6
St.15	2.1	20.6	2.59	87	0.24	11.7
St.16	7.5	90.4	12.8	270	0.83	322.9
St.17	9.6	95.3	19.1	300	1.1	1733.9
St.18	6.8	83.8	13.8	300	0.88	3453.5
St.19	7.6	96.6	13.4	140	0.57	72.8
St.20	7.5	72.3	13.4	960	1.6	552.5
St.21	10.9	98.8	22.8	300	0.69	5579.0
St.22	7.3	94.4	12.7	200	0.53	708.8
St.23	7.5	96.1	13.9	200	0.50	588.5
St.24	7.1	97.0	12.4	140	0.36	197.2
St.25	6.1	97.6	10.2	130	0.39	42.0
St.26	5.1	85.9	8.95	160	0.39	188.2
St.27	4.9	61.8	8.59	180	0.45	630.4
St.28	4.5	45.3	7.24	220	0.53	181.3
St.29	5.6	80.2	8.64	190	0.49	424.7
St.30	3.9	46.9	5.29	99	0.21	79.6
St.31	4.6	58.7	6.34	93	0.21	32.8
St.32	2.1	7.9	2.22	70	0.14	6.5
St.33	2.1	12.4	2.07	84	0.19	3.7
St.34	6.7	99.0	10.2	140	0.38	85.2
St.35	7.9	99.4	11.8	150	0.48	41.5

3. Adsorption experiment on PAHs

Experiments of the adsorption in an anaerobic condition of PAHs using the sediment samles of St. 1, St,2, St.4, St9, St.12, St.17, St.18, St.27, St.31, and St.33 were conducted.

(1)Materials and methods

The adsorption characteristics of the sediments of the Nagoya port were investigated in a laboratory experiment. In the batch adsorption test, 0.1g-wet sediment, 0.5g-wet sediment, and 1g-wet sediment and 50mL artificial sea water, and 500μL of PAHs standard solution with the concentration of 20mg/L (initial concentration was 0.2mg/L), were added and then stirred at 100rpm for 48hours. The tests were performed in a dark environment and at a constant temperature (25 ± 1 ℃) to minimize possible losses of the target compounds by photodegradation and evaporation. The slurry was centrifuged at 2,000 rpm for 5 minutes in the first stage of the experiment. The supernatant liquid were then filtered with a glass fiver filter (1μm), and the dissolved phase was separated from the solids phase.

The PAHs concentration in the solid phase was measured by heated alkaline solvent extraction method. The PAHs concentration in the dissolved phase was measured as follows. The filtratated solution was decanted to a separationf funnel. 10mL of Hesane was poured into the funnel, and the

internal standard solution of deuterated PAHs was added, and then shaken for 5 min. The extracted hexane solution was concentrated under 60℃ under nitrogen gas stream. The concentrated solution was then analyzed by GC/MS.

The PAHs concentrations in the dissolved phase (C_w) and the solid phase (C_s) were then determined, and the partition coefficient ($K_p = C_s / C_w$) was calculated. The control samples without solids were processed in the same manner as above.

(2)Results and discussion

Fig.2-Fig.11 shows the differences of Kp of the PAHs for each sample in the adsorption experiments. Although the result on the soil sample taken at St.18 showed a opposite tendency, Kp was increased with the increase in the hydrophobicity of the compounds. Consequently, the hydrophobic compounds had a greater ability to be adsorbed in the sediments than the hydrophilic compounds.

Fig.12-Fig.21 show the plots of Log Kp against Log Kow in the case of different sediments used in the experiments. An expression for the empirical relation between Kp and Kow can be written as follows.

$$Log_{10}K_p = a \cdot Log_{10}K_{ow} + b \qquad (1)$$

where a and b are constants. The constant *a* expresses the effect of K_{ow} and the constant b expresses the characteristic of sediments depending on the soil property. The relations between K_{ow} and K_p from the adsorption experiments are illustrated in **Fig. 12** – **Fig. 21**, where the lateral axis denotes Log K_{ow}, and the vertical axis denotes Log K_p. The results show that a substance with the more intensive hydrophobic characteristic was distributed more to the particulate phase. The correlation between K_{ow} and K_p was observed in the experimental results, except for samples of St.12, St.18, and St.33. The equations for the relation between K_p and K_{ow} for individual samples are following.

$St.1: \quad Log_{10}K_p = 1.1099 \cdot Log_{10}K_{ow} - 5.1993$

$St.2: \quad Log_{10}K_p = 1.5586 \cdot Log_{10}K_{ow} - 7.4059$

$St.4: \quad Log_{10}K_p = 0.9702 \cdot Log_{10}K_{ow} - 4.1805$

$St.9: \quad Log_{10}K_p = 1.3937 \cdot Log_{10}K_{ow} - 6.6089$

$St.12: \quad Log_{10}K_p = 0.6918 \cdot Log_{10}K_{ow} - 3.4744$

$St.17: \quad Log_{10}K_p = 1.2604 \cdot Log_{10}K_{ow} - 5.4992$

$St.18: \quad Log_{10}K_p = -1.0154 \cdot Log_{10}K_{ow} + 4.9848$

$St.27: \quad Log_{10}K_p = 1.6581 \cdot Log_{10}K_{ow} - 7.5933$

$St.31: \quad Log_{10}K_p = 1.3314 \cdot Log_{10}K_{ow} - 5.6183$

$St.33: \quad Log_{10}K_p = 1.1222 \cdot Log_{10}K_{ow} - 4.1448$

The slopes in the equations are in a range 0.97 – 1.65, except for St.12, St.18, and St.33. The intercepts are in a range 4.1805 – 7.5933. It means that the order of K_p differes three orders depending on the samples It is hence confirmed that Kp is strongly influenced by the properties of the samples.

4. One-dimension deffusion model

A one-dimensional diffusion model was applied to estimate the leaching of PAHs in a long period.

(1) Outline of the model

Equation 3 is the one-dimensional diffusion equation of chemicals in sediments.

$$n \cdot \frac{\partial C_w}{\partial t} + (1-n) \cdot \rho_s \cdot \frac{\partial C_s}{\partial t} = n \cdot D_z \cdot \frac{\partial^2 C_w}{\partial z^2} - \lambda \cdot \left[n \cdot C_w + (1-n) \cdot \rho_s \cdot C_s \right] \qquad (3)$$

where C_w is concentration of dissolved material, C_s is concentratioin of absorved matrial, n is porosity, ρ_s is density of sediment particle, D_s is coefficient of diffusion, and λ is diospersion rate.

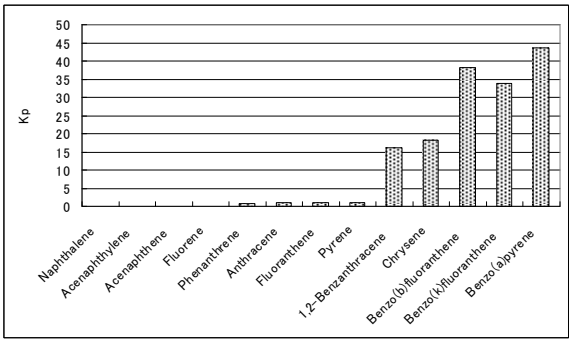

Fig.2 The difference of Kp of the PAHs at St.1

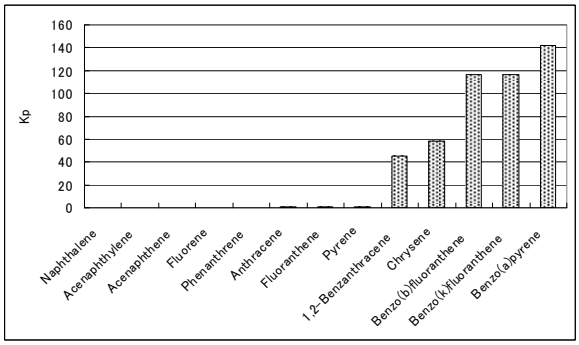

Fig.3 The difference of Kp of the PAHs at St.2

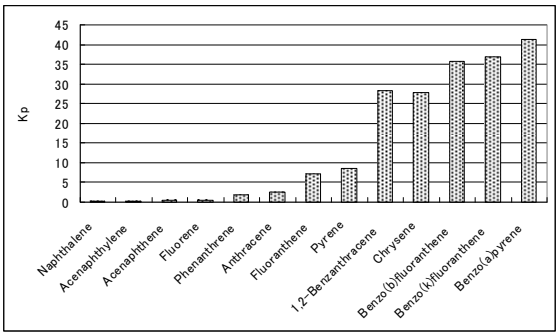

Fig.4 The difference of Kp of the PAHs at St.4

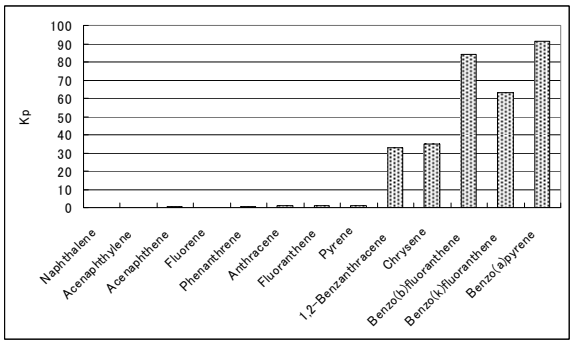

Fig.5 The difference of Kp of the PAHs at St.9

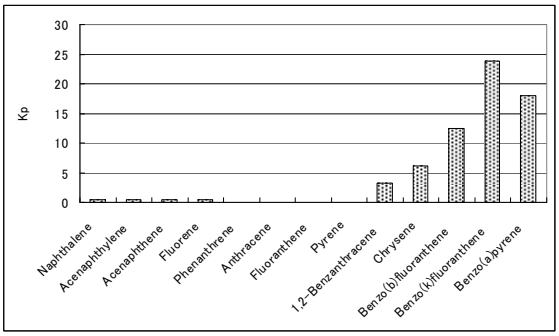

Fig.6 The difference of Kp of the PAHs at St.12

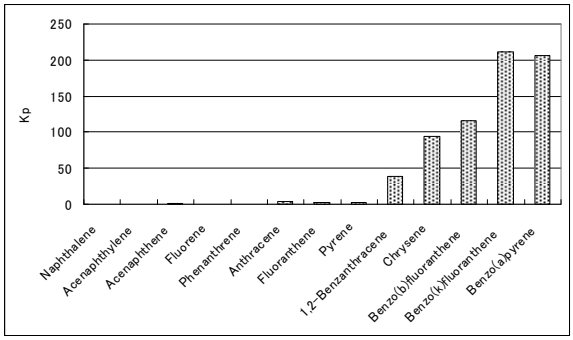

Fig.7 The difference of Kp of the PAHs at St.17

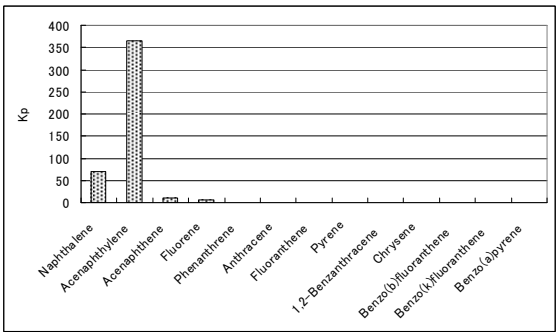

Fig.8 The difference of Kp of the PAHs at St.18

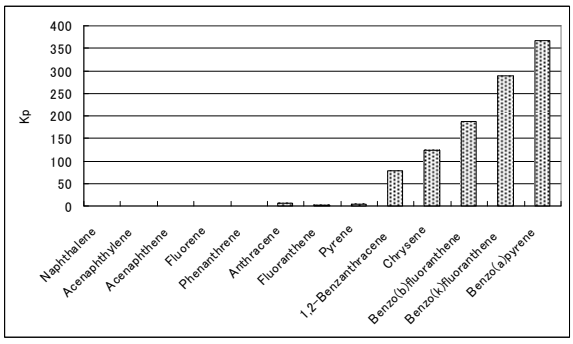

Fig.9 The difference of Kp of the PAHs at St.27

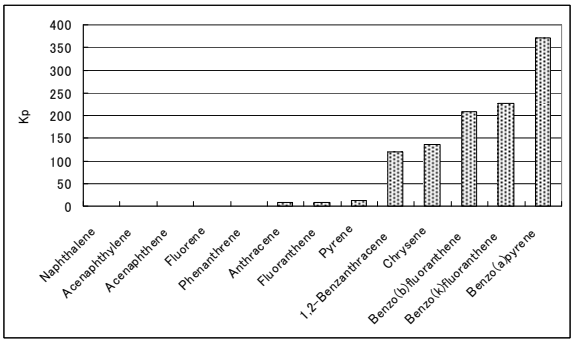

Fig.10 The difference of Kp of the PAHs at St.31

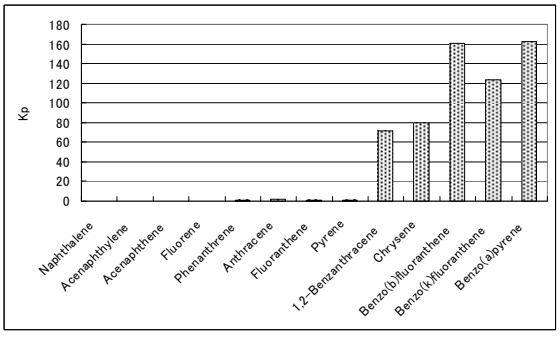

Fig.11 The difference of Kp of the PAHs at St.33

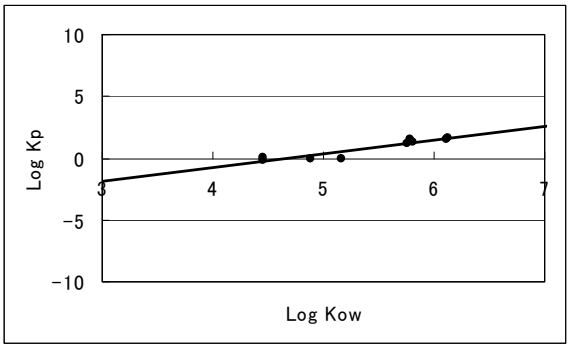

Fig.12 The plots of Log Kp against Log Kow with sediment of St.1

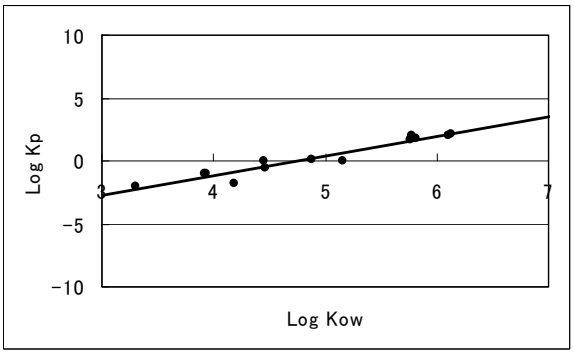

Fig.13 The plots of Log Kp against Log Kow with sediment of St.2

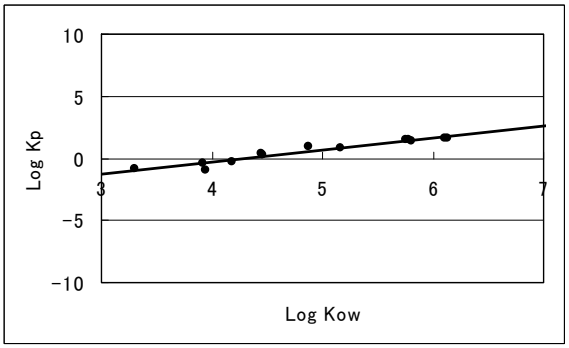

Fig.14 The plots of Log Kp against Log Kow with sediment of St.4

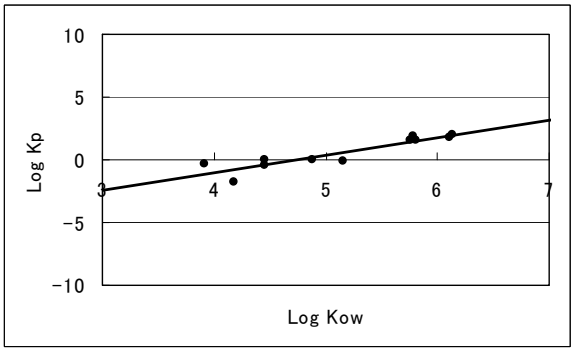

Fig.15 The plots of Log Kp against Log Kow with sediment of St.9

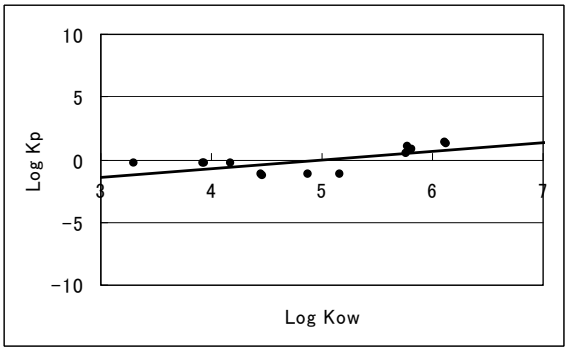

Fig.16 The plots of Log Kp against Log Kow with sediment of St.12

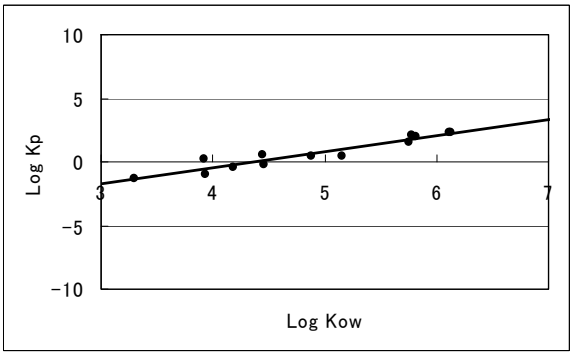

Fig.17 The plots of Log Kp against Log Kow with sediment of St.17

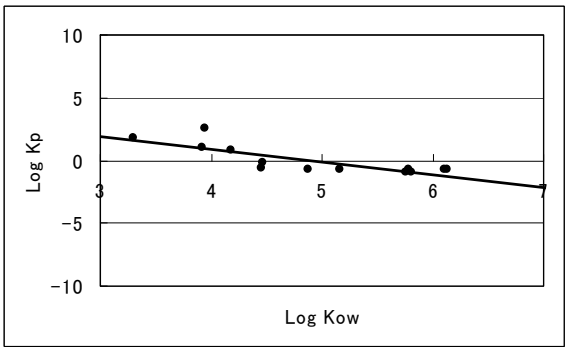

Fig.18 The plots of Log Kp against Log Kow with sediment of St.18

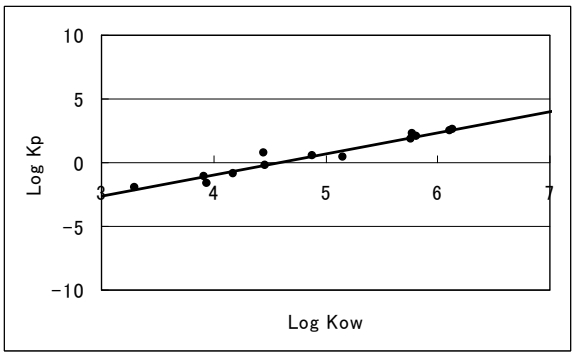

Fig.19 The plots of Log Kp against Log Kow with sediment of St.27

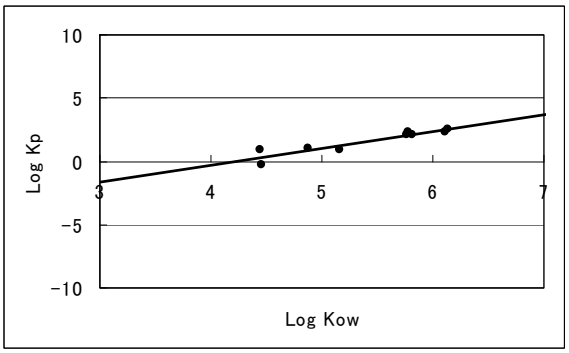

Fig.20 The plots of Log Kp against Log Kow with sediment of St.31

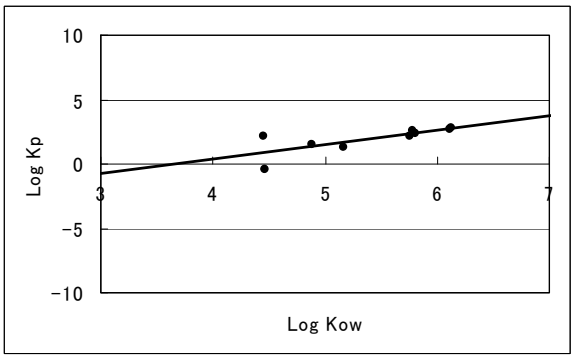

Fig.21 The plots of Log Kp against Log Kow with sediment of St.33

C_s and R (retardation coefficient) are expressed by the following equations.

$$C_s = K_p \cdot C_w$$

$$K_p = IL \cdot K_{om} \qquad (4)$$

$$R = 1 + \frac{1-n}{n} \cdot \rho_s \cdot K_p$$

where K_p is the partition coefficient between the splid phase and the dissolved phase, IL is ignition loss, K_{om} is the partition coefficient between ignition loss and water. Now, equation 3 is simplified to the following equation 5.

$$\frac{\partial C_w}{\partial t} = \frac{D_z}{R} \cdot \frac{\partial^2 C_w}{\partial z^2} - \lambda \cdot C_w \quad (5)$$

The target samples for the numerical analysis by using equation (5) are sediment of St. 2, which contained the least amount of loss on ingintion, and that of St.9, contained the highest loss on ignition. The target materials in the analysis were benzo(a)pyrene, which is hydrophobic and has the highest moleculer weight, and naphthalene, which is hydrophilic and has the lowest moleculer weight, and fluoranthene has the intermediate moleculer weight. The diffusion coefficient was estimated by equation (6), which Oya et al. used.

$$D_z = 8.76 \times 10^{-9} (M_W)^{-0.48} \quad (6),$$

in which, M_w is moleculer weight. The porosity and the density of sediment particles in the calculation were the measured values in the filed trip. Kom was evaluated by EPI suite software.

(2) Results and discussion

Fig.22 and Fig.23 show the results of numerical analysis of the diffusion of benzo(a)pyrene. Those results show that benzo(a)pyrene spread in the capping layers over time in both cases of different capping materials containing different amounts of loss on ignition. In the case of the soil sample with higher loss on ignition, the amount of leaching is

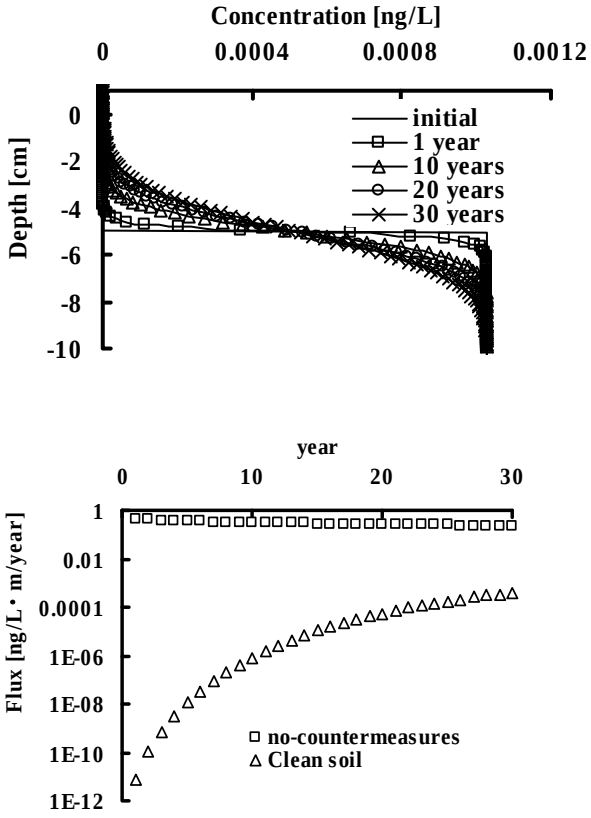

Fig.22Vertical distribution of benzo(a)pyrene from the contaminated soil with high organic content capped by the seidiment of St.9 and leaching flux

0.18% of that in the case without capping, and in the case of the soil sample with lower loss on ignition, the leaching was 0.96% of the case without capping.

Those results show that the capping with materials that show the less amount of loss on inginition than 1% can reduce the leaching amount of benzo(a)pyrene less than 1% of the case without capping.

Fig. 24 and Fig. 25 show the results of the numeriucal analysis of the diffusion of naphthalene. In the case of naphthalene, which has the lowest Kp, the efficiency of the capping is almost lost in the first one year, and the ability to reduce diffusion of materials is not sufficient in any case.

Fig.26 and Fig 27 show the results of the vertical distribution of the concentration and the leqaching flux over years of the fluoranthene case, respectively. The results shown in Fig.26, in both cases of capping materials with different amounts of loss on ignition indicated that the capping is effective for the reduction of leaching for the first ten years. However, the effectiveness of capping gradually decreases with time elapsed. The leaching flux in figure 27 shows that the capping with the materials of the high loss on ignition can reduce the leaching amount of fluoranthene to the 16% of that of the case without capping, thirty years later. However, the capping with the materials of the lower loss on ignition can only reduce the leaching amount to 49.1% of the case without capping during the same period. Those results imply that the capping with the materials of the higher loss on ignition is expected to have the high efficiency for the reduction of the long-term leaching of fluoranthene.

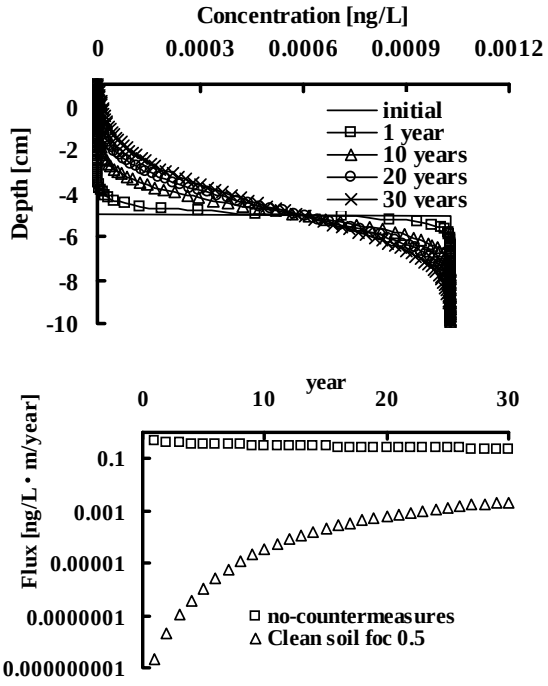

Fig.23 Vertical distribution of benzo(a)pyrene from the contaminated soil with high organic content capped by the seidiment of St.2 and leaching flux

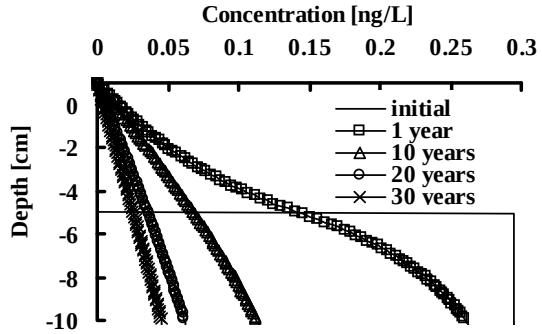

Fig.24 Vertical distribution of naphthalene from the contaminated soil with high organic content capped by the seidiment of St.9

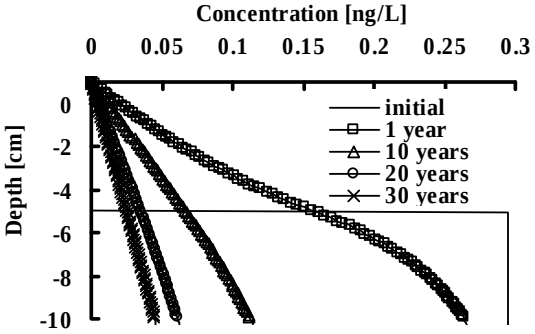

Fig.25 Vertical distribution of naphthalene from the contaminated soil with high organic content capped by the seidiment of St.2

5. Conclusion

1) The results of the field observation in Nagoya port show that samples from the vicinity of the river mouth of the Horikawa River have the characteritics of high loss on ignition, high TOC, high zinc and cadmium concentrations. Those concentrations have an tendency to decrease with the distance from the river mouth. Those results imply that the sources of zinc and cadmium in sediments are similar for those of TOC and they are discharged from the urbanized area of Nagoya city.

2) The tendency that the PAHs of high moleculer weight are easily adsorved by sediments is confirmed by the coefficients of partition. By the least square method, linear relationships between log Kp and log Kow was obtained for different soil samples.

3) The analysis using the one-dimensionl diffusion model show following results: The reduction of the leaching of hydrophilic materials, such as naphtharene, is difficult by the capping because those materlas are easy to be distributed in the water phase; The capping is expected to be effective for the reduction of the leaching of hydrophobic compounds, such as benzo(a)pyrene because those materlas are easy to be adsorved in the soil; the long term efficiency of the capping on the reduction of the leaching of the intermediate molecular weight compounds with moderate hydrophobicity depends on the ignition loss of the material used for the capping.

References

[1]Toshiharu Hirose, Keiko Morito, Ryoichi Kizu, Akira Toriba,Kazuichi Hayakawa, Sumito Ogawa, Satoshi Inoue, Masami Muramatsu, and Yukito Masamune. Estrogenic/Antiestrogenic Activities of Benzo(a)pyrene Monohy7droxy Derivatives. Journal of Health Science 2001, 47 (6),552-558

[2]Makiko Kamiya, Akira Tobira, Yu Onoda, Ryuichi Kizu, Kazuichi Hayakawa. Evaluation of edtrogenic activities of hydroxylated polycyclic aromatic hydrocarbons in cigarette smoke condensate. Food and Chemical Toxicology 2005, 43, 1017-1027

[3]Heike Kaupp, and Michael S. Mclachlan. Gas/Particulate partitioning of PCDD/Fs, PCBs, PCNs and PAHs. Chemosphere 1999, Vol. 38, No. 14,3411-3421

[4]R.K. Aryal, H.Furumai,F.Nakajima,M.Boller. Dynamic behavior of fractional suspended solids and particle-bound polycyclic aromatic hydrocarbons in highway rnoff.Water Research 2005, 39, 5126-5134

[5]Haruhiko Oya, Akihito Haio, Youichi Negishi, Mikinao Mtsumoto (1990): Standardization of ultrafiltlation membrane, Membrane (Japanese membrane academy magazine), 15, 2 ,62-71.

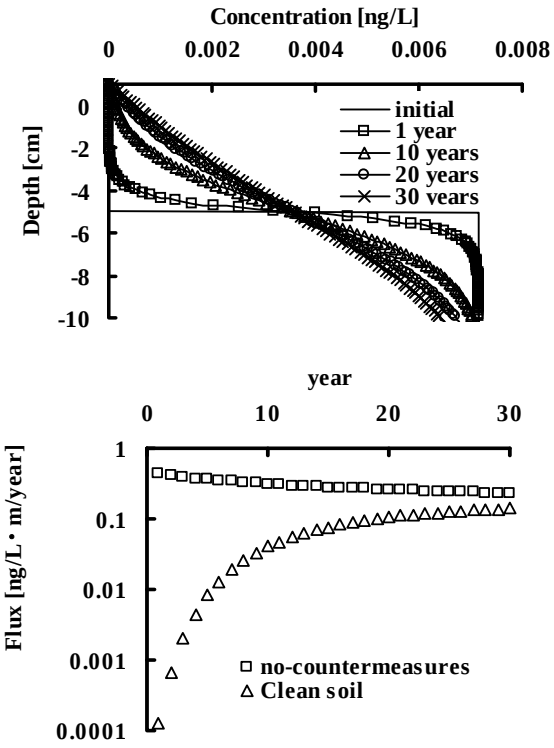

Fig.26 Vertical distribution of fluoranthene from the contaminated soil with high organic content capped by the seidiment of St.9 and leaching flux

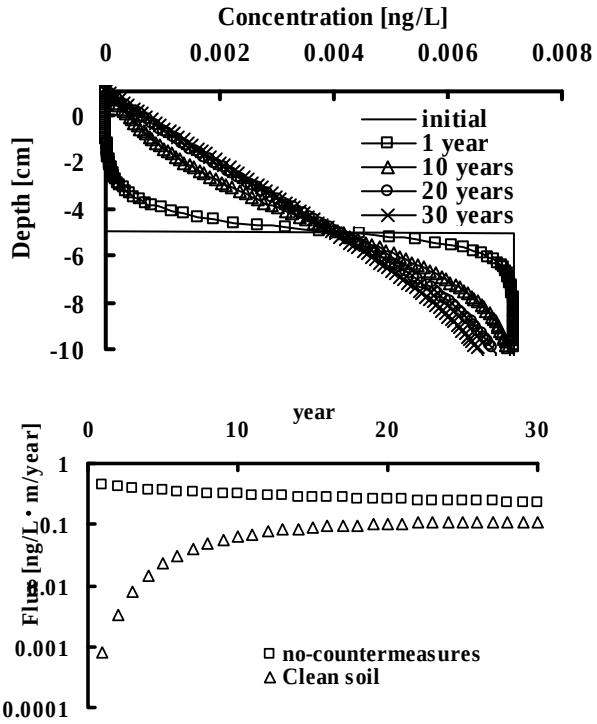

Fig.27 Vertical distribution of fluoranthene from the contaminated soil with high organic content capped by the seidiment of St.2 and leaching flux